2008 IEEE International Conference on RFID
The Venetian, Las Vegas, Nevada, USA
April 16-17, 2008

A Printed Rampart-Line Antenna with a Dielectric Superstrate for UHF RFID Applications

Benjamin D. Braaten, *Student Member, IEEE,* Gregory J. Owen, *Student Member, IEEE,* Dustin Vaselaar, *Student Member, IEEE,* Robert M. Nelson, *Senior Member, IEEE,* Cherish Bauer-Reich, *Student Member, IEEE,* Jacob Glower, *Member, IEEE,* Brian Morlock, *Member, IEEE,* Michael Reich, *Member, IEEE,* and Aaron Reinholz, *Member, IEEE*

***Abstract*— A printed Rampart line antenna with a dielectric superstrate for passive Radio Frequency Identification (RFID) tags is presented. A design process is outlined to determine the number of elements used in the Rampart line antenna to achieve the required gain for the desired read range. An inductive loop is then added to the port to match the antenna with the passive tag circuitry. It is shown that a passive tag with a printed Rampart line antenna and a dielectric superstrate can achieve comparable read ranges to commercially available passive RFID tags.**

I. INTRODUCTION

Interest in Radio Frequency Identification (RFID) systems has grown tremendously in the past few years [1]-[5]. Literature exists on everything from supply chain management [6]-[8] to RFID security [9]-[10] and from UHF antenna design [11] to back-scattering analysis of RFID tags [12]-[14]. Two major characteristics that distinguish different types of RFID systems are the power source of the tag and the frequency of operation [1]. A good review of different types of RFID systems can be found in [1]. A strictly passive RFID system uses the energy from the field radiated by the reader to completely power the (passive) tags. The tag then uses this energy to identify itself and communicate with the reader. A tag in this system typically has an antenna attached to a rectifier circuit to provide a voltage and current that will power the tag circuitry. At high frequencies it is the relation between the input impedance of the rectifier circuit and the antenna impedance and gain that will play a major role in the read range of the tag [12].

It is well known that the gain, input impedance and resonant frequency of an antenna can be affected by nearby conducting and non-conducting objects [15]-[16]. In particular, it has been shown that a microstrip antenna with several substrates and a superstrate of isotropic and anisotropic material can be significantly effected by the material properties and layer thickness [17]-[21]. These material properties and layer thicknesses can effect the input impedance [17],[19] and the resonant frequency [18],[20] of a microstrip antenna. But several advantages are gained by using a superstrate over the microstrip antenna. The superstrate can provide protection against heat, physical damage, the environment and also increases the peak power-handling capability of the antenna [18]. For example, if a passive RFID tag is attached to a car for electronic tolling [22] or to cattle for tracking [23]-[24] it may have a dielectric cover for weatherproofing. The image in Figure 1 is an ear tag for cattle with a passive RFID tag embedded in the material. The material completely enclosing the tag protects the tag from the environment and provides a means of attaching the tag to the animal. In this case the material above the tag can be modeled as a dielectric superstrate. It is the intent of this paper to present an antenna design with a desired input impedance and gain for a passive UHF RFID tag with a dielectric superstrate. However a brief review of the relationship between the read range and antenna characteristics of a passive RFID tag is presented.

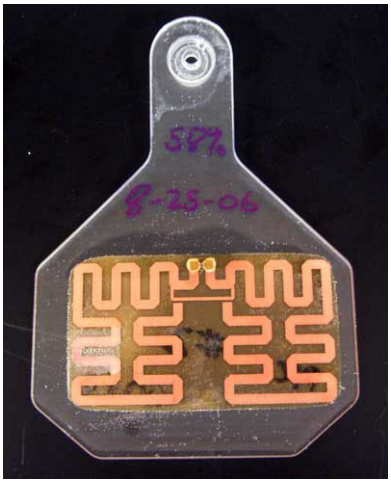

Fig. 1. Cattle tag with embedded passive RFID tag.

The max theoretical read range r_{max} between a reader and a passive RFID tag can be written using Friis's equation as [25]

$$r_{max} = \frac{\lambda}{4\pi}\sqrt{\frac{P_t G_t G_r (1-|s|^2)}{P_{th}}} \quad (1)$$

where λ is the free space wavelength, P_t is the transmit power, G_t is the gain of the transmitting antenna (reader

This work was supported by the Center for Nanoscale Science and Engineering (CNSE) at North Dakota State University, Fargo ND, 58102.

B.D. Braaten, G.J. Owen, R.M. Nelson, C. Bauer-Reich, and J. Glower are with the Electrical and Computer Engineering Department at North Dakota State University, Fargo ND, 58102. (email: benbraaten@ieee.org)

D. Vaselaar, M. Reich, and A. Reinholz are with the Center for Nanoscale Science and Engineering (CNSE) at North Dakota State University, Fargo ND, 58102.

B. Morlock is with Packet Digital LLC, Fargo ND, 58102.

antenna), G_r is the gain of the receiving antenna (tag antenna), P_{th} is the minimum power required to power the tag, and

$$|s|^2 = \left| \frac{Z_L - Z_A^*}{Z_L + Z_A} \right|^2 \quad (2)$$

is the power reflection coefficient. In (2) the load impedance (tag rectifier input impedance) is denoted as Z_L and the antenna impedance is denoted as Z_A. We can see in (1) that r_{max} depends on two parameters of the tag antenna: $|s|^2$ and G_r. Thus it is possible to improve the read range between the reader and passive tag by minimizing (2) and maximizing G_r.

Typically a designer involved with the layout process of a passive RFID tag has a planar surface on which to place the antenna, which usually leads to a printed antenna design. One major difficulty is to design an antenna with the correct combination of G_r and $|s|^2$ that provides the desired read range on a very limited surface area. The next section presents a design method for a planar printed antenna with high space-filling characteristics, various values of G_r and a large range of Z_A. This is then used as a tool to design an antenna for a passive tag with a dielectric superstrate. It should be noted that this design process will work for Gen 1 and 2 [26] printed antennas on passive RFID tags without dielectric superstrates.

II. ANTENNA DESIGN PROCESS

In general we have the possible layout region described in Figure 2. The region around the strap is the area allowed for the printed antenna. At this point the two requirements of the antenna are a desired input impedance and gain. Thus there exists an extremely large amount of possible layouts in the allocated region for the antenna [27]-[30] and in some cases a ground plane may or may not be present or the designer may be required to place the antenna on many different surfaces [31]-[37]. Two popular antenna designs for RFID tags are a meander line dipole [38],[11] and a long triangular dipole [12]. These antennas provide very good read ranges but the dimensions may be too large for some applications (9cm-11cm wide). Two more recent antenna designs for RFID tags are an inductively coupled antenna at 910MHz [39] and a meander-slot antenna [40]. The inductively coupled antenna design is very small (4cm x 4.6cm) and has a nearly isotropic radiation pattern. The meander-slot antenna is optimized using a genetic algorithm and has a dimension of 5cm x 5cm. Even though the previous two antennas are very small, some cases may require a larger gain to achieve further read ranges. Other UHF antenna work has focused on optimization based on genetic algorithms [41] and numerical electromagnetic code (NEC) to simulate all possible layouts of a meander line antenna [38]. The design method presented here has only been tested on antennas that do not have a ground plane. The authors believe that the method will also yield helpful information for other systems.

First, start with the antenna in Figure 3 a). This is a Rampart line antenna [29] with N elements on each pole. The first step in the iterative design process is to determine

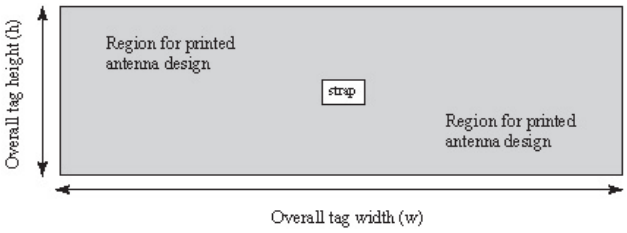

Fig. 2. Possible tag layout region.

the electrical width and length of the Rampart line antenna. To do this consider the individual element of the Rampart line antenna in Figure 3 b). We have labeled the starting and ending nodes of the k^{th} element as e_{k-1} and e_k, respectively. The other nodes of interest in the design process have been labeled as a_k, b_k, c_k and d_k. Next, we will denote the electrical length between any two nodes, say x and y, in Figure 3 b) as $L^e_{x,y}$. Using this notation we denote the electrical length between nodes e_{k-1} and a_k as $L^e_{e_{k-1},a_k}$. In a similar manner, we can write the electrical length between the remaining nodes as $L^e_{a_k,b_k}$, $L^e_{b_k,c_k}$, $L^e_{c_k,d_k}$ and $L^e_{d_k,e_k}$. Thus the electrical length of the entire k^{th} segment is

$$L^e_k = L^e_{e_{k-1},a_k} + L^e_{a_k,b_k} + L^e_{b_k,c_k} + L^e_{c_k,d_k} + L^e_{d_k,e_k}. \quad (3)$$

Therefore, the electrical length of the one pole of the dipole is

$$L^e_p = \sum_{n=1}^{N} L^e_n \quad (4)$$

where L^e_n=$L^e_{e_{n-1},a_n}$+$L^e_{a_n,b_n}$+ $L^e_{b_n,c_n}$+ $L^e_{c_n,d_n}$+$L^e_{d_n,e_n}$. This then gives the entire length of the dipole as

$$L^e_d = \sum_{n=-N,n\neq 0}^{N} L^e_n. \quad (5)$$

Note that (5) is written without any assumptions on the symmetry of each element. It is written, however, with the assumption that the dipole is symmetric about the port. If we define some symmetry on the elements of the Rampart line antenna we can simplify (3). If we allow $S^e_k = L^e_{e_{k-1},a_k} = L^e_{a_k,b_k} = L^e_{c_k,d_k} = L^e_{d_k,e_k}$ in Figure 3 b) we reduce (3) to

$$\tilde{L}^e_k = 4S^e_k + L^e_{b_k,c_k}. \quad (6)$$

This then gives the overall dipole length of

$$L^e_d = \sum_{n=-N,n\neq 0}^{N} \tilde{L}^e_n. \quad (7)$$

For the rest of this paper we will assume the symmetry that leads to the expression in (6). For example, if we defined $S^e_k = \lambda/32$ and $L^e_{b_k,c_k} = \lambda/8$ we get $\tilde{L}^e_k = \lambda/4$ which gives an overall dipole length of $L^e_d = N\lambda/2$.

The next step in the design process is to determine the number of elements N in each pole of the dipole. This is done by first fixing the center frequency f_o and adding elements symmetrically about the port location until a maximum gain is achieved (input impedance will be designed for

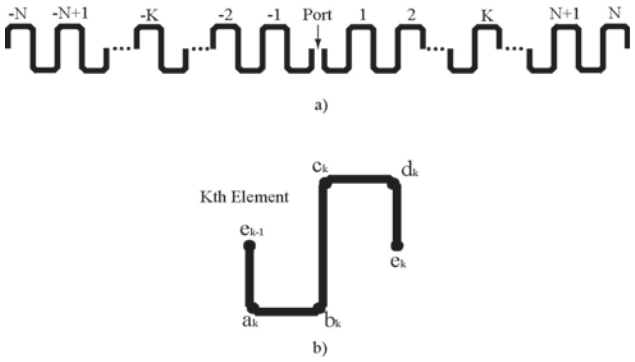

Fig. 3. Rampart line antenna layout.

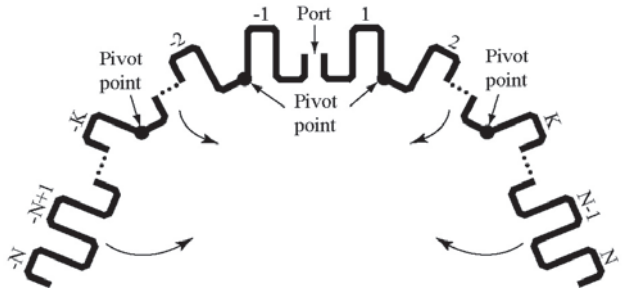

Fig. 4. Pivoting the Rampart line antenna.

later). Usually elements can be added until the gain reaches a maximum and when more elements are added the gain is reduced. Once the gain starts degrading, remove elements to achieve the maximum gain. CAD programs work nicely for determining N for many applications. N depends on the environment around the passive tag during use. Thus, if N is determined for a specific operating frequency in free space and the antenna is used with a substrate, then N may not provide the desired gain in this application.

Once the desired N in the Rampart line antenna has been determined we need to fit the antenna in the area allocated for it on the tag. Typically N is so large that it won't fit in the required area. To fit the antenna we define pivot points at various segment junctions along the antenna. The process of defining these pivot points and moving the appropriate segments around on the antenna plane is illustrated in Figure 4. In this case each arm of the dipole has two pivot points defined. One on the second segment of each pole and one on the K^{th} segment (for illustration of the general procedure) of each pole. Defining the pivot points in appropriate locations allows the designer to fit the originally long Rampart line antenna onto a much smaller area in a very efficient space-filling manner. Results from our research seem to indicate that only a small sacrifice in gain is given to fit the antenna on the tag.

To design for a desired input impedance of the antenna an inductive loop is added to the port of the antenna in Figure 4. A direct method of determining the width, length and location of the loop is not presented but it was noticed that the further away the loop was from the port the higher the

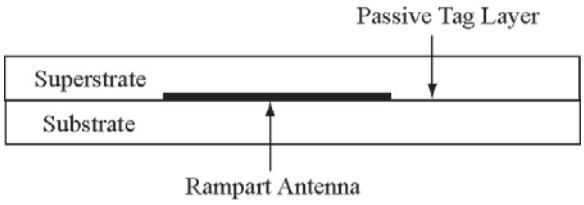

Fig. 5. Passive tag with superstrate.

gain. Typically the loop for this design process is placed between the first two elements ($N = \pm 1$) of the Rampart line antenna. The inductive loop was used to control the reactance of Z_A. The width of the antenna traces were used to control the resistance of Z_A. Thus, by adjusting the inductive loop and width of the traces Z_A could take on many different values. To illustrate this design method we will consider the following printed antenna for a UHF passive RFID tag with a dielectric superstrate.

III. ANTENNA DESIGN

In this design a printed Rampart line antenna with a dielectric superstrate is evaluated using Advanced Design System (ADS) by Agilent [42]. The operating frequency f_o is 920MHz with a 60 mil substrate with ε_r=4.25 and a 60 mil superstrate of ε_r=4.0. The placement of the antenna is shown in Figure 5.

To determine the value of N, elements were added symmetrically about the port location. It was determined that for this f_o the max gain occurred with twelve elements on each pole. Thus, for the design presented here we chose N=12 for a G_r=4.3dBi. The Rampart line antenna was then shortened a bit and folded six times to fit on the space provided for the tag. This lead to the designs in Figure 6. We have added an inductive loop at the terminals of the folded Rampart line antenna to conjugate match the antenna port impedance with the load. The layout in Figure 6 a) has a gain of G_r=2.62dBi and input impedance of $Z_{in,a}$=10.527+j139.263. The dimensions are H=2985mils, W=1522mils and a trace width of 100mils. The layout in Figure 6 b) has a gain of G_r=2.97dBi and input impedance of $Z_{in,b}$=36.93+j139.737. The dimensions are H=2746mils, W=1540mils and a trace width of 150mils. Notice that $Z_{in,b}$ has a larger real part. This is believed to be a result of the wider trace providing a larger radiation resistance. We can see that increasing the number of elements of each pole fills the antenna space more and allows the antenna to be bent to fit on the tag. This utilizes the limited antenna space more efficiently.

The designs in Figure 6 were manufactured on printed on 5mils FR4 and BT substrate. The images of the two layouts are shown in Figure 7 a) and b). The design in Figure 7 a) shows the layout with the narrow trace width on the FR4 substrate. Figure 7 b) shows the layout with the wider trace width on the BT substrate. Type F and type PFC conductive epoxy made by Epotec [43] was used to attach the straps on the designs in Figure 7 a) and b). The epoxy for all tags

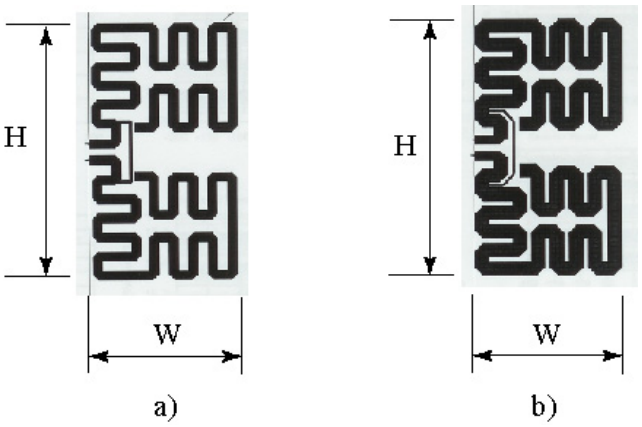

Fig. 6. (a) Rampart line antenna with superstrate and narrow trace (b) Rampart line antenna with superstrate and wide trace .

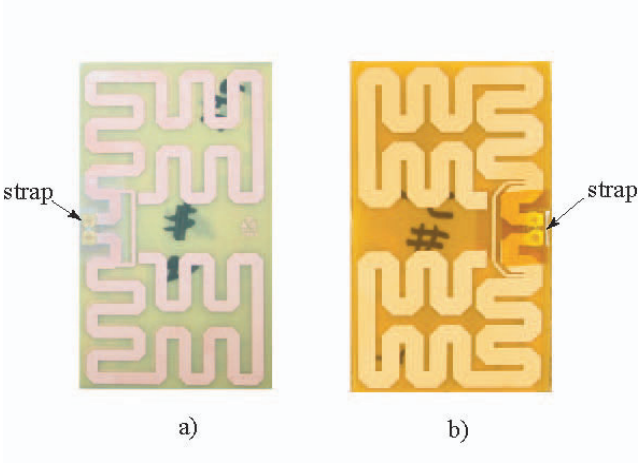

Fig. 7. (a) Layout with narrow trace from board manufacturer on 5mil substrate (b) Layout with wide trace from board manufacturer on 5mil substrate.

was cured at 50^{o}C for 8hrs. Both layouts (wide and narrow trace) were printed on both types of substrates (FR4 and BT). This resulted in four different types of printed antennas. The combination of printed antennas and two different types of epoxy (type F and PFC) resulted in eight variations, which were all tested.

IV. MEASUREMENT RESULTS

To test the new designs the structure in Figure 8 was constructed. The foam piece that holds the RFID tag can vary in height (H) as 3ft$\leq H \leq$17ft. An Alien technology 9780 Gen 1 reader [44] with a linearly polarized (LP) antenna and 4W of effective radiated power was placed on the ground below the tag. For a benchmark, the read range of the commercially available M-tag from Alien was determined. The read range was defined as the point when the read rate changed *from* the max read rate *to* a lower read rate (either a marginal read rate or zero). The M-tag was placed in the foam without a dielectric substrate and superstrate, yielding a read range of 13.5ft. When the M-tag was placed in the

Fig. 8. Antenna test structure (highest).

foam with the dielectric substrate and superstrate of 60mil and ε_r=4.0 the read range was reduced to 8.5ft. This is a 37 percent reduction in read range for passive RFID tags not designed for a superstrate (i.e. enclosure) which illustrates why commercially available tags need to be designed for the presence of superstrates.

Next, the layouts in Figure 7 were placed between the dielectric layers and the read range for various tags were recorded. The values for these tests are in Table I. We can see that a max read range of 10.5ft is achieved for the layout in Figure 7 a) on the FR4 substrate with type F epoxy.

For the results in Table II the LP antenna on the Alien technology reader was replaced with a circularly polarized (CP) antenna. Again, the M-tag was placed in the foam with the dielectric substrate and superstrate and the read range was reduced to 6.5ft. We can see that a max read range of 7.5ft is achieved for the layout in Figure 7 a) on the FR4 substrate with type F epoxy. In both cases a larger read range than the commercially available passive tag was achieved.

Various radiation properties of the layouts in Figure 7 a) and b) were simulated in ADS and measured using the Alien reader. The pattern was determined with the reader by measuring the max read range of the tag with respect to angle. This method of correlating read range and pattern has been shown by Yang [45] to accurately represent the field pattern. During these experiments the tag was kept in the far field to correlate the max read range with attenuation of the reader [46]. It is assumed that the tag is in the x-y plane

TABLE I

READ RANGE TEST RESULTS FOR LINEARLY POLARIZED ANTENNA.

Layout in Figure 7	a)	b)	a)	b)
5mil substrate type	FR4	FR4	BT	BT
Read range (F epoxy)	10.5ft	5.5ft	10.5ft	5ft
Read range (PFC epoxy)	9.5ft	5.5ft	8.5ft	6ft

TABLE II

READ RANGE TEST RESULTS FOR CIRCULARLY POLARIZED ANTENNA.

Layout in Figure 7	a)	b)	a)	b)
5mil substrate type	FR4	FR4	BT	BT
Read range (F epoxy)	7ft	<4ft	7.5ft	4ft
Read range (PFC epoxy)	7.5ft	<4ft	6.5ft	4.5ft

of the spherical coordinate system with the dimension H measured along the y-axis. The angle θ is measured from the positive z-axis and the angle ϕ is measured from the positive x-axis. For the results in Figures 9-17 the value of θ was swept from 0 to 360^o and ϕ is fixed at 0^o and 90^o (at the positive x-axis and y-axis, respectively). We can see in Figures 9 and 10 that the θ component of the field is fairly uniform in the y-z plane and agree well with the measurements taken by the Alien reader. The results in Figures 11 and 12 show the magnitude of the total field in the y-z plane. This shows that the θ component of the electric field is the dominant component in y-z plane. The results in Figures 13-16 show the ϕ component and the magnitude of the total field for a cut angle of $\phi = 0^o$ (x-z plane). This shows that the dominant term in the x-z plane is the ϕ component. Finally, we can see in Figure 17 that layout b) has a larger gain. The input impedance of the antenna was simulated using ADS and is shown in Figure 18. The top plot shows that the real part of the input impedance can be increased by increasing the trace width. We can also see that the input impedance of the antenna changes very little over the band 850Mhz to 950Mhz, which is the frequency of interest. This is useful for matching over the frequency hopping spectrum used by the reader.

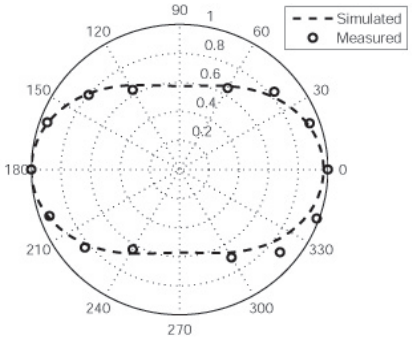

Fig. 9. Normalized pattern of E_θ for layout a) at 920MHz for $\phi = 90^o$ and $0 \leq \theta \leq 360^o$.

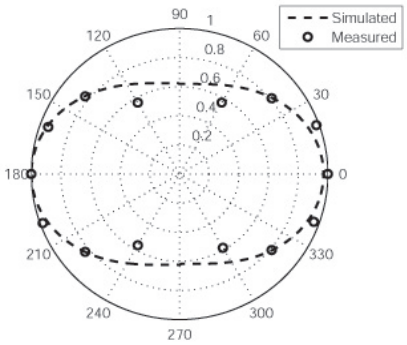

Fig. 10. Normalized pattern of E_θ for layout b) at 920MHz for $\phi = 90^o$ and $0 \leq \theta \leq 360^o$.

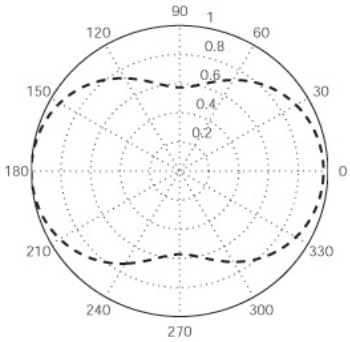

Fig. 11. Simulated normalized pattern of $|E_{total}|$ for layout a) at 920MHz for $\phi = 90^o$ and $0 \leq \theta \leq 360^o$.

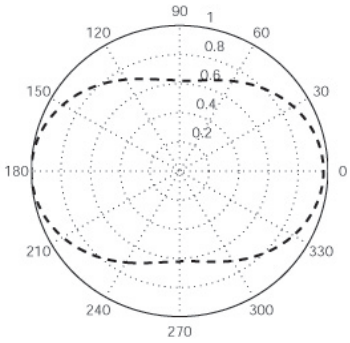

Fig. 12. Simulated normalized pattern of $|E_{total}|$ for layout b) at 920MHz for $\phi = 90^o$ and $0 \leq \theta \leq 360^o$.

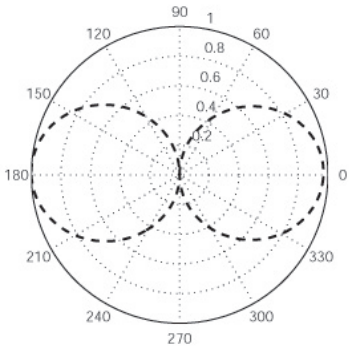

Fig. 13. Simulated normalized pattern of E_ϕ for layout a) at 920MHz for $\phi = 0^o$ and $0 \leq \theta \leq 360^o$.

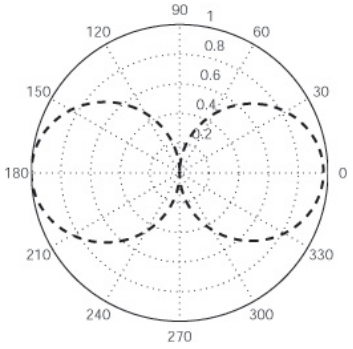

Fig. 14. Simulated normalized pattern of E_ϕ for layout b) at 920MHz for $\phi = 0^o$ and $0 \leq \theta \leq 360^o$.

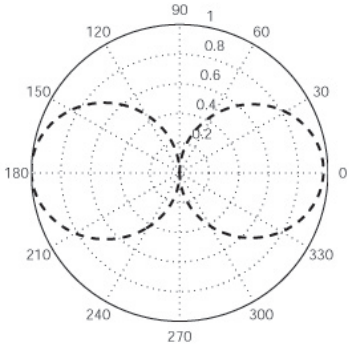

Fig. 15. Simulated normalized pattern of $|E_{total}|$ for layout a) at 920MHz for $\phi = 0^o$ and $0 \leq \theta \leq 360^o$.

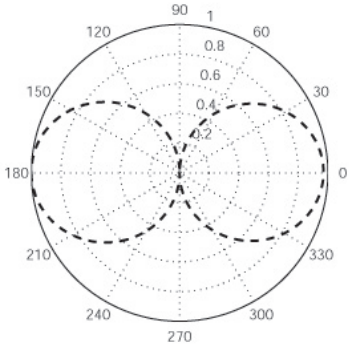

Fig. 16. Simulated normalized pattern of $|E_{total}|$ for layout b) at 920MHz for $\phi = 0^o$ and $0 \leq \theta \leq 360^o$.

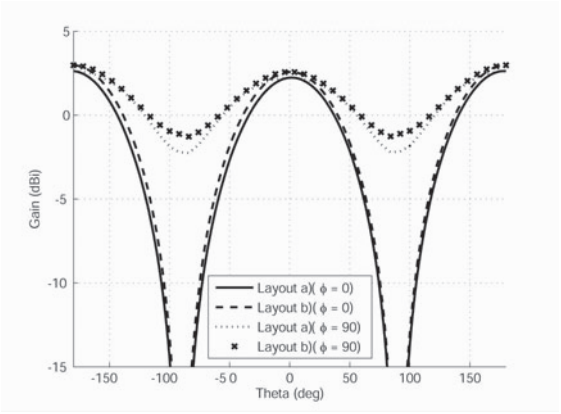

Fig. 17. Simulated gain in dB for layout a) and b) at 920MHz for $\phi = 0^o$ and $\phi = 90^o$ and $0 \leq \theta \leq 360^o$.

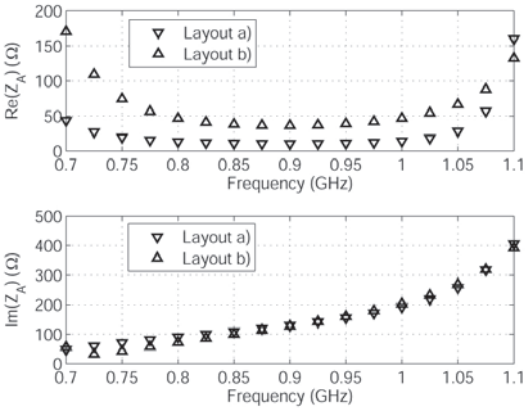

Fig. 18. Simulated input impedance.

V. CONCLUSION

A design process based on the Rampart line antenna has been presented. This process yields antennas with high gain values, flexibility in input impedance design, high space filling properties and essentially a constant input impedance over the frequency band of interest. Two antenna designs with very similar gain values and input impedance are presented. It is shown that antennas with dielectric superstrates can be designed for passive RFID tags that yield read ranges larger than commercially available tags.

REFERENCES

[1] K. Finkenzeller, *RFID Handbook:Fundamentals and Applications in Contactless Smart Cards and Identification*, John Wiley and Sons, West Sussex, England, 2003.

[2] J.-P. Curty, M. Declercq, C. Dehollain and N. Joehl, *Design and Optimization of Passive UHF RFID Systems*, Springer-Verlag New York, LLC, 2006.

[3] E. Cooney, *RFID+:The Complete Review of Radio Frequency Identification*, Cengage Delmar Learning, 2006.

[4] D. Paret, R. Riesco and R. Riesco, *RFID and Contactless Smart Card Applications*, John Wiley and Sons, Inc., 2005.

[5] V.D. Hunt, A. Puglia and M. Puglia, *RFID-A Guide to Radio Frequency Identification*, John Wiley and Sons, Inc., 2007.

[6] E.W. Schuster, S.J. Allen and D.L. Brock, *Global RFID: The Value of the EPCglobal Network for Supply Chain Management*, Springer-Verlag New York, LLC, 2006.

[7] L. Boglione, "RFID Technology - Are you ready for it?", IEEE Microwave Magazine, Vol. 8, No. 6, December 2007, pp. 30-32.

[8] R.A. Kleist, D.A. Sakai, B.S. Jarvis, T. Chapman and D. Sakai, *RFID Labeling: Smart Labeling Concepts and Applications for the Consumer Packaged Goods Supply Chain*, Banta Book Group, 2005.

[9] B. Rosenberg, *RFID: Applications, Security, and Privacy*, Pearson Education, 2006.

[10] F. Thornton, B.R. Haines, A. Das, A. Campbell and B. Haines, *RFID Security*, Syngress Publishing, 2006

[11] K.V.S. Rao, P.V. Nikitin and S.F. Lam, "Antenna Design for UHF RFID Tags: A Review and a Practical Application," *IEEE Transactions On Antennas and Propagation,* Vol. 53, No. 12, December 2005, pp. 3870-3876.

[12] C.-C. Yen, A.E. Gutierrez, D. Veeramani, and D. van der Weide, "Radar Cross-Section Analysis for Backscattering RFID Tags," *IEEE Antennas and Wireless Propagation Letters,* Vol. 6, 2007, pp. 279-281.

[13] B.D. Braaten, Y. Feng and R.M. Nelson, "High-frequency RFID tags: an analytical and numerical approach for determining the induced currents and scattered fields," *IEEE International Symposium on Electromagnetic Compatibility,* August 14-18, 2006, pp.58-62.

[14] Y. Feng, B.D. Braaten and R.M. Nelson, "Analytical expressions for small loop antennas-with application to EMC and RFID systems," *IEEE International Symposium on Electromagnetic Compatibility,* August 14-18, 2006, pp.63-68.

[15] C.A. Balanis, *Antenna Theory: Analysis and Design*, Harper and Row, Publishers, New York, 1982.

[16] W.L. Stutzman and G.A. Thiele, *Antenna Theory and Design*, 2nd ed., John Wiley and Sons, Inc., New York, 1998.

[17] V. Hansen and M. Patzold, "Input impecdance and mutual coupling of rectangular microstrip patch antennas with a dielectric cover," *16th European Microwave Conference, 1986,* October 1986, pp. 643-648.

[18] I.J. Bahl, P. Bhartia and S.S. Stuchly, "Design of microstrip antennas covered with a dielectric layer," *IEEE Transactions on Antennas and Propagation,* Vol. 30, No. 2, March 1982, pp. 314-318.

[19] J.R.S. Oliveira and A.G. D'Assuncao, "Input impedance of microstrip patch antennas on anisotropic dielectric substrates," *Antennas and Propagation Society International Symposium, 1996. AP-S. Digest,* Vol. 2, July 21-26, 1996, pp. 1066-1069.

[20] R.M. Nelson, D.A. Rogers and A.G. D'Assuncao, "Resonant frequency of a rectangular microstrip patch on several uniaxial substrates," *IEEE Transactions on Antennas and Propagation,* Vol. 38, No. 7, July 1990, pp. 973-981.

[21] A.K. Verma and Nasimuddin, "Input impedance of rectangular microstrip patch antenna with iso/anisotropic substrate-superstrate," *IEEE Microwave and Wireless Components Letters,* Vol. 11, No. 11, November 2001, pp. 456-458.

[22] P. Blythe, "RFID for road tolling, road-use pricing and vehicle access control," *IEE Colloquium on RFID Technology (Ref. No. 1999/123),* Oct. 25, 1999, pp. 811-816.

[23] RFID Journal, www.rfidjournal.com.

[24] M.L. Ng, K.S. Leong, D.M. Hall and P.H. Cole, "A small passive UHF RFID tag for livestock identification," *IEEE International Symposium on Microwave, Antenna, Propagation and EMC Technologies for Wireless Communications, 2005*, Vol. 1, Aug. 8-12, 2005, pp. 67-70.

[25] P.V. Nikitin, K.V.S. Rao, S.F. Lam, V. Pillai, R. Martinez, and H. Heinrich "Power Reflection Coefficient Analysis for Complex Impedances in RFID Tag Design," *IEEE Transactions On Microwave Theory and Techniques,* Vol. 53, No. 9, September 2005.

[26] EPC Global, www.epcglobalinc.org.

[27] A. Sundaram, M. Maddela and R. Ramados, "Koch-Fractal Folded-Slot Antenna Characteristics," *IEEE Antennas and Wireless Propagation Letters,* Vol. 6, 2007, pp. 219-222.

[28] K.-L. Wong, C.-H. Chang, and Y.-C. Lin, "Printed PIFA EM Compatible with Nearby Conducting Elements," *IEEE Transactions on Antennas and Propagation,* Vol. 55, No. 10, October 2007, pp. 2919-2922.

[29] I.J. Bahl and P. Bhartia, *Microstrip Antennas*, Artech House, Inc. Dedham, MA, 1980, pp.214-215.

[30] D.M. Pozar and D.H. Schaubert, *Microstrip Antennas: The analysis and Design of Microstrip Antennas and Arrays*, IEEE Press, Piscataway, NJ, 1995.

[31] S.S. Basat, S. Bhattacharya, L. Yang, A. Rida, M.M. Tentzeris, J. Laskar, "Design of a novel high-efficiency UHF RFID antenna on flexible LCP substrate with high read-range capability," *IEEE Antennas and Propagation Society International Symposium,* July 9-14, 2006, pp.1031-1034.

[32] C.T. Rodenbeck "Planar miniature RFID antennas suitable for integration with batteries," *IEEE Transactions on Antennas and Propagation,* Vol. 54, No. 12, December 2006, pp. 3700-3706.

[33] Q. Jinghui, S. Bo, Y. Qidi, "Study on RFID antenna for railway vehicle identification," *6th International Conference on ITS Telecommunications Proceedings,* June, 2006, pp.237-240.

[34] M. Stupf, R. Mittra, J. Yeo and J.R. Mosig, "Some novel design for RFID antennas and their performance enhancement with metamaterials," *IEEE Antennas and Propagation Society International Symposium 2006,* July 9-14, 2006, pp.1023-1026.

[35] S.Y. Leung, D.C.C. Lam, "Performance of printed polymer-based RFID antenna on curvilinear surface," *IEEE Transactions on Electronics Packaging Manufacturing,* Vol. 30, Issue 3, July 2007, pp. 200-205.

[36] G. Marrocco, "RFID antennas for the UHF remote monitoring of human bodies," *IET Seminar on Antennas and Propagation for Body-Centric Wireless Communications,* April 24, 2007, pp. 51-56.

[37] D. Bechevet, T.-P. Vuong and S. Tedjini, "Design and measurements of antennas for RFID, made by conductive ink on plastics," *IEEE Antennas and Propagation Society International Symposium 2005,* July 3-8, 2005, pp.345-348.

[38] A. Galehdar, D.V. Thiel and S.G. O'Keefe, "Antenna efficiency calculations for electrically small, RFID antennas," *IEEE Antennas and Wireless Propagation Letters,* Vol. 6, 2007, pp. 156-159.

[39] J. Ahn, H. Jang, H. Moon, J.-W. Lee and B. Lee, "Inductively coupled compact RFID tag antenna at 910MHz with near-isotropic radar cross-section (RCS) patterns," *IEEE Antennas and Wireless Propagation Letters,* Vol. 6, 2007, pp. 518-520.

[40] C. Calabrese and G. Marrocco, "Meandered-slot antennas for sensor-RFID tags," *IEEE Antennas and Wireless Propagation Letters,* Vol. 7, 2008, pp. 5-8.

[41] G. Kim and Y. Chung, "Optimization of UHF RFID tag antennas," *IEEE Antennas and Propagation Society International Symposium 2006,* July 9-14, 2006, pp. 2087-2090.

[42] Agilent Technologies, *www.agilent.com*

[43] www.epotec.info/

[44] Alien Techology, *www.alientechnology.com*

[45] L. Yang, A. Rida, R. Vyas and M.M. Tentzeris, "RFID tag and RF structures on a paper substrate using inkjet-printing technology," *IEEE Transactions On Microwave Theory and Techniques,* Vol. 55, No. 12, December 2007, pp. 2894-2901.

[46] P.V. Nikitin, K.V.S. Rao and S. Lazar, "An overview of near field UHF RFID," *IEEE International Conference on RFID, 2007,* March 26-28, 2007, pp. 176-174.